Original Study **Open Access**

Włodzimierz Brząkała*

Stress-weighted spatial averaging of random fields in geotechnical risk assessment

https://doi.org/10.2478/sgem-2021-0039
received July 28, 2021; accepted November 22, 2021.

Abstract: Effects of spatial fluctuations of soil parameters are considered in a new context – considering variability of soil parameters in conjunction with non-uniform stress fields, which can locally amplify (or suppress) subsoil inhomogeneities. In this way, several design situations for the Coulomb frictional material with random $\tan(\varphi(x))$ reveal a reduction of variance, which is less significant than for the standard volume averaging. When looking for an 'effective' random variable $[\tan(\varphi)]_a$ – that is, a random variable, which is equivalent to the random field $\tan(\varphi(\underline{x}))$ – the Vanmarcke averaging by simple volume integrals is insufficient; it systematically overestimates effects of variance reduction, thus causing potentially unsafe situations. The new proposed approach is coherent, formally defined and more realistic.

Keywords: spatial variability; effective soil parameters; variance reduction; the Vanmarcke averaging; safety factor.

1 Introduction

Reliability-based design methods have recently been widely applied to geoengineering, in which the spatial variability of soil parameters (random fields) plays an important role. Early studies from the late 60s focused on random stability of slopes. The first models considered soil strength parameters as spatial random fields; however, simple random variables are more useful in practical applications (EN 1997-1; Low and Phoon 2015, Tietje et al. 2011). Recent risk analyses widely implement random data as spatial random fields of auto- and crosscorrelated parameters or even use complete probabilistic definition with joint probability distributions (Ching et al. 2016, Javankhoshdel and Bathurst 2015, Griffith and Fenton 2001, Jiang et al. 2015, Shen et al. 2021). Data acquisition and operations on such spatial data require sophisticated numerical support, but – alternatively – some techniques of data pre-processed simplifications are also effective; the former direction can be found in some selected papers attached as references (Cho 2007, Deng et al. 2017, Farah et al. 2015, Ji et al. 2018, Jiang et al. 2014, Kim and Sitar 2013, Li et al. 2017, Liu et al. 2017, Liu et al. 2018, Shen 2021, Tietje et al. 2011), while the latter direction is presented hereafter.

Another group of boundary problems analyses random bearing capacity of footings in a random field context focusing on the most important regions, where shear resistance is generated along slip lines or slip surfaces. The undrained conditions are often analysed (frictionless materials, the Tresca model), which do not depend on stresses (Chwała 2019, Griffith and Fenton 2001, Huang et al. 2013, Li et al. 2015, Puła and Chwała 2015, Shen et al. 2021). For frictional or frictional–cohesive materials, the situation is more complex because stress fields cannot be ignored (Fenton and Griffith 2003, Liu et al. 2017).

Modelling of input data as spatial random fields complicates risk analyses; therefore, advanced analytical or numerical methods are widely in use. The fundamental difficulty is that such sophisticated models, often parameter sensitive, should be in a balance with high quality of geoengineering input data and the data look never complete; that is why, for practical design situations, the random models are sometimes reduced from spatial random fields to simple random variables (Vanmarcke 2010, Low and Phoon 2015) by making use of some averaging techniques. Note that the spatial averaging does not necessarily mean that any significant part of information is lost. In a context of interactions between adjacent regions in a subsoil mass, significant up and down fluctuations of random parameters can reduce each other; so, the volume averaging of spatially distributed soil parameters is rationally justified and economical – it reduces point variances of considered random fields (Tietje

***Corresponding author: Włodzimierz Brząkała,** Department of Geotechnics, Hydroengineering, Underground- and Water-Structures, Wroclaw University of Science and Technology, Wyb. Wyspianskiego 27, 50-370 Wroclaw, Poland, E-mail: wlodzimierz.brzakala@pwr.edu.pl

Open Access. © 2021 Włodzimierz Brząkała, published by Sciendo. This work is licensed under the Creative Commons Attribution alone 4.0 License.

et al. 2011). In addition, the method of spatial averaging has a strong mathematical background (Vanmarcke 2010) as well as a variety of well-documented applications.

The paper focuses mainly on the subsoil shearing resistance – like $\tau = q_n \times \tan(\varphi)$ for the frictional Coulomb material – and analyses the variance reduction coefficients γ_a for the homogeneous random field $\tan(\varphi(\underline{x}))$, which is reduced by averaging to a corresponding random variable $[\tan(\varphi)]_a$. Fields of stresses in the subsoil mass implement a new element to the averaging procedures because non-uniform (deterministic) normal stresses $q_n \neq \text{const}(\underline{x})$ generate a kind of subsoil inhomogeneities, in terms of the random shearing resistance $\tau(\underline{x})$. Indeed, if a normal stress q_n along a slip line is locally negligible, then $\tau = q_n \times \tan(\varphi)$ is also locally negligible and such a region does not contribute to total bearing capacity. If locally $q_n \sim 0$ in shearing resistance, then the friction coefficient $\tan(\varphi)$ is locally not very important and especially its random fluctuations $\Delta\tan(\varphi)$ can be ignored; also, it is vice versa for a locally concentrated load $q_n >> 0$. Vanmarcke's spatial averaging applied to soil strength parameters (or to soil deformation parameters) ignores this mechanism and this is controversial. Clearly, the Vanmarcke averaging of spatial random fields is effective for many 'stress-neutral' random parameters like radioactive radiation, pollutant concentration, temperature, etc. For example, the spatial geometrical averaging is very useful in hydrological studies – hydrologists evaluate average rainfalls over a certain geographical region to estimate flood danger in an entire river basin (Vanmarcke 2010); but this model is insufficient for ultimate limit states, which are based on a random field $\tan(\varphi(\underline{x}))$ because the Coulomb shearing resistance τ is additionally 'disturbed' by spatially distributed normal loads $q_n(\underline{x})$.

It is assumed that the spatial field of the normal stress $q_n(\underline{x})$ is deterministic and physically independent of the random field $\tan(\varphi(\underline{x}))$. The stress field $q_n(\underline{x})$ plays the role of a fourth source of inhomogeneity – apart from the inherent one, from deterministic trends and measurement/transformation errors – because the stress field $q_n(\underline{x})$ can amplify (or suppress) effects of random local fluctuations. A new point of view on the spatial averaging of random fields in geoengineering is presented below, and the paper's objectives focus on simple numerical examples. The paper implements a more general and coherent concept of averaging of random fields and allows a conclusion that the standard (purely geometrical) variance reduction based only on volume integrals can be too optimistic; in a context of geotechnical structural safety, the traditional volume averaging can be dangerous.

Only few papers consider in a distinct way volume averaging in conjunction with fields of stresses, though there is a widespread agreement that the spatial regions being close to loaded places play a pivotal role in the averaging; being 'close to loaded places' means not only a short distance, but also local stress components of a maximal intensity. Recently, it was found by Ching and Hu (2017) and Ching et al. (2016) that the traditional spatial averaging model that treats all soil regions equally important cannot satisfactorily represent the effective Young modulus for the footing settlement problem – highly mobilised soil regions close to a footing are more significant than non-mobilised ones; the authors proposed some weight coefficients derived from a random finite element analysis. Similarly, for random shearing resistance of a rectangular sample analysed via finite elements (Ching and Phoon 2013), the authors found that the averaging over the whole sample overestimates the variance reduction, whereas the averaging along slip lines is much more representative; such a conclusion for localised shearing resistance should not be surprising. In the next paper, the authors confirmed this conclusion for a wider class of boundary problems (Ching et al. 2016).

2 Soil parameters as random variables

Soils display inherent inhomogeneities caused by long-term geological processes, unknown stress history, soil moisture, chemical reactions, etc.; therefore, soil parameters have a random nature, which can be described in terms of random variables or spatial random fields (time effects are not considered hereafter). Such local random fluctuations that happen *in situ* can be amplified during soil parameter evaluation, that is, by soil testing (usually invasive), measurement errors, calibration procedures, transformation models and others (Phoon and Kulhawy 1999a, 1999b); therefore, in geotechnical risk assessment, the term uncertainty of geotechnical parameters is more adequate than the term inherent inhomogeneity. Reported fluctuations of geotechnical parameters are relatively great, much greater than in cases of man-made construction materials. Considering a subsoil layer as a macro-homogeneous mass, the uncertainty can be expressed using coefficients of variations (c.o.v.) called $\nu = \sigma/\mu$, so a standard deviation σ over an expected value $\mu > 0$. This distribution-free parameter is the minimal information about subsoil uncertainty; it can be sufficient only in simple practical applications.

Numerous authors present the results, literature reviews and discussions on 'typical' values of c.o.v. (%), like the values reviewed by Phoon and Kulhawy (1999a). Clearly, the data from many countries, regions, geological units, climate zones and even from different geological companies differ substantially and may be incomparable. This explains inevitable discrepancies in published data. Reported c.o.v. are sometimes based on estimated inherent inhomogeneity, but sometimes they are based on a total uncertainty that includes measurement errors, etc. Moreover, algorithms of de-trending can be different, non-standard testing procedures and individual data transformation methods are sometimes implemented (Phoon and Kulhawy 1999a). For an illustrative character of this paragraph, generalised 'most typical' values can be derived based on the review papers by Phoon and Kulhawy (1999a, 1999b): for the internal friction coefficient $\nu_{\tan(\varphi)} \sim$ 5%–15% (non-cohesive soils), $\nu_{\tan(\varphi)} \sim 25\%$ (cohesive soils, even up to 50% is possible; slightly less for the angle φ itself), for the cohesion $\nu_c \sim$ 20%–30% (for undrained shear strength, even up to 70% is possible) and for the deformation modulus $\nu_D \sim$ 30%–50%. The presented values refer to the mean values of inherent variability; the intervals for global uncertainty can be still wider, at least 10%–20% due to measurement errors.

The following negative crosscorrelation coefficient is usually reported: $-0.75 < r_{\tan(\varphi);c} < 0$ and the value $r_{\tan(\varphi);c} \sim -0.3$ can be recommended as a conservative estimation. Note that deterministic physical arguments do not always confirm the assumed negative crosscorrelation between φ or $\tan(\varphi)$ and c. Indeed, local fluctuations of soil moisture cause simultaneous decrease (or increase) of both $\tan(\varphi)$ and c; this fact can support suggestion about a positive correlation. On the other hand, local fluctuations of fine particle content result in random changes of $\tan(\varphi)$, which are simultaneously opposite to changes of c; this fact can support the conclusion about a negative correlation. Tests on drained and undrained samples also suggest a negative correlation ($c_u > c'$, $\varphi_u \sim 0^o < \varphi'$). A review of previous papers and study on the role of negative crosscorrelation can be found in Javankhoshdel and Bathurst (2015).

Reliability-based design methods that use only the random variable format can cause an overdesign of foundations or other geoengineering structures. There are several possible reasons for this: ultimate limit state conditions may be oversimplified (too restrictive), some improvements of soil parameters may happen during construction, the database about geotechnical failures may be still poor – or the values of the c.o.v. may be 'too large', even though they are correct as point estimations. Indeed, it is a well-established fact that point variances $Var\{P(\underline{x})\} = \sigma^2 = \text{const}(\underline{x})$ of a homogeneous random field of soil parameters $P(\underline{x})$ are usually not representative (overestimated) in geotechnical safety analyses because they ignore the interactions between adjacent regions in the considered soil mass. Bearing in mind dimensions of such adjacent regions – expressed in metres or dozens of metres – local random fluctuations can compensate each other in a considered soil mass as a whole, if total (summarised) effects are of interest. Formally, these are autocorrelation and crosscorrelation functions (between different parameters), which cause such reduction effects. This observation is a pivot of the monographies by Vanmarcke (2010, 1983) and numerous next papers.

Simple reliability models based on random variables that use only the expected values μ and standard deviations σ – instead of spatial random fields of subsoil parameters – are the most popular tool in safety evaluation, including the Eurocodes (EN 1997-1). In this context, a special attention is paid to averaging techniques called as spatial random homogenisation or volume integrals, which can transform spatially fluctuating random fields to some equivalent random variables. Since for a homogeneous random field, the expected value $E\{P(\underline{x})\} = \mu = \text{const}$, any spatial averaging will not change this value, but the averaging yields an 'effective' variance $Var_a = \gamma_a \times \sigma^2$ with a reduction coefficient $\gamma_a \leq 1$; equivalently, but in terms of standard deviations $\sigma_a = \Gamma_a \times \sigma$, therefore, the symbol $\Gamma_a = \sqrt{\gamma_a}$ is also in use (Vanmarcke 2010, Tietje et al. 2011).

3 Soil parameters as random fields

Consider a homogeneous random field of a soil parameter (or several soil parameters in a vectorial version) denoted as $P(\underline{x})$, where a point $\underline{x} = (x_1, ..., x_n)$ belongs to a domain $D \subset E^n$ in n-dimensional Euclidean space. The assumed homogeneity means that for every two points $\underline{x}$, $\underline{y}$, the expected values and the variances of two random variables $P(\underline{x})$, $P(\underline{y})$ are the same, $E\{P(\underline{x})\} = E\{P(\underline{y})\} = \mu = \text{const}$, $Var\{P(\underline{x})\} = Var\{P(\underline{y})\} = \sigma^2 = \text{const} < +\infty$; the covariance function equals $Cov\{P(\underline{x});P(\underline{y})\} = E\{[P(\underline{x}) - \mu] \times [P(\underline{y}) - \mu]\} = \sigma^2 \times \rho(\underline{x} - \underline{y})$, so the corresponding correlation coefficient ρ depends only on the difference $\Delta\underline{x} = \underline{x} - \underline{y}$ or simply $\rho = \rho(\Delta\underline{x})$. Note that the approach is also effective for some quasi-homogeneous random fields when homogeneous random fluctuations happen around a functional deterministic trend $\mu + f(\underline{x})$, like for a subsoil stiffness and strength which often increase with depth (Li et al. 2015). In principle, the homogeneity requirement concerns the homogeneous random fluctuations and not so much deterministic trends; so, during the pre-processing, the

model should be de-trended (Bagińska et al. 2016, Li et al. 2015). Another technique is used by Shen et al. (2021); the authors recommend a modulating amplitude $A(\underline{x})$, which is a deterministic function, but modifies the considered random field of subsoil parameters $P(\underline{x}) = A(\underline{x}) \times H(\underline{x})$. The randomness is still generated by a homogeneous random field $H(\underline{x})$. In particular, subsoil resistance derived from vertical cone penetration tests (CPT) can have the form of a stochastic process $q_c(z)$ with increasing both the expected value and the standard deviation (proportionally), but the model is not more complicated.

Joint probability distributions of the random field $P(\underline{x})$ are not specified, if the simplest distribution-free second-order model is used. Moreover, it is assumed that the probabilistic averaging (ensemble averaging) and spatial averaging (volume averaging) coincide. This is only a useful hypothesis that cannot be proved in frames of distribution-free theories. In geotechnical practice of soil testing, one cannot carry out any sequence of independent measurements at the same point – the list of fully non-invasive geotechnical tests is very short. Replacing the term 'at the same point' by a more liberal 'at the same place' can be controversial; this difficulty leads to multiscale models, ambiguous definitions of 'representative volume elements' (Ostoja-Starzewski 2006) and nested micro–meso inhomogeneous models (Jaksa et al. 1999, Ching and Phoon 2013), which are not discussed here.

Several types of the decay functions $\rho(\Delta\underline{x})$ became popular; four of them are discussed in detail by Vanmarcke (2010), Bagińska et al. (2016) and Oguz et al. (2019), the squared exponential (Gaussian) in particular (equation 1a). Due to natural sedimentation processes over vast areas, the geological model of the subsoil can reveal a horizontally layered structure like for transversally isotropic continua; hence, the following squared exponential representation of the correlation function $\rho(\underline{x};\underline{y}) = \rho(\underline{x} - \underline{y})$ is useful:

$$\rho = \exp\left\{-\frac{(x_1-y_1)^2+(x_2-y_2)^2}{(d_h)^2}\right\} \cdot \exp\left\{-\frac{(x_3-y_3)^2}{(d_v)^2}\right\} \quad (1a)$$

where the symbols x_3, y_3, d_v are used for vertical direction. Alternatively, the linear exponential (Markovian) function (equation 1b) is in use:

$$\rho = \exp\left\{-\frac{|x_1-y_1|+|x_2-y_2|}{d_{h'}}\right\} \cdot \exp\left\{-\frac{|x_3-y_3|}{d_{v'}}\right\} \quad (1b)$$

Although the equations (1a) and (1b) apply to general 3D situations, the points of interest $\underline{x}$, $\underline{y}$ are often situated on certain specific subsets like along slide lines (surfaces) in ultimate limit states or limit equilibrium studies.

In data processing, sometimes a negative autocorrelation can happen that is beyond the scope of the exponential functions (1a and 1b); if such negative values are not incidental, and so if they are confirmed by significance tests, then a wider class of cosine exponents like $\exp\{-|\Delta x|/d'\} \times \cos(|\Delta x|/d'')$ can be considered. Such a 'more chaotic' behaviour seems to be possible for anthropogenic soils, for example for lignite mine dumping soils (Bagińska et al. 2016) or low-quality sandy backfills (Brząkała, 1981); in the former case, averaged locally negative values up to $\rho \sim -0.2$ are reported (but not used, assumed $d'' = +\infty$) and in the latter one, the values are up to $\rho \sim -0.5$ (horizontal variability of a subsoil vertical response over a meso-scale laboratory field 4.2 m × 2.0 m, several dozens of testing points). The problem of negative autocorrelation for nearshore sea bottom soils is recently discussed by Oguz et al. (2019). The values derived from CPT tests in stiff, overconsolidated clays can also be negative (up to $\rho \sim -0.2$) (Jaksa et al. 1999). In the context of risk assessment and averaging, note that ignoring the negative values of ρ is usually on the safe side (Fig. 1b).

The decay constants d_v, d_h (m) in equation (1a) control the speed of convergence to zero for increasing distances and they are in close relation to so-called scales of fluctuations δ_i (Vanmarcke 2010, Bagińska et al. 2016, Pieczyńska-Kozłowska et al. 2017, Tietje et al. 2011), which are good intuitive measures of random fluctuations. The following definitions of δ and δ' are in use for unidirectional random variations due to equations (1a) and (1b), respectively:

$$\delta = \int_{-\infty}^{+\infty} \rho(r)dr = \int_{-\infty}^{+\infty} \exp\left(-\frac{r^2}{d^2}\right) dr = \sqrt{\pi}\, d \quad (2a)$$

$$\delta' = \int_{-\infty}^{+\infty} \rho(r)dr = 2\int_{0}^{+\infty} \exp\left(-\frac{r}{d'}\right) dr = 2d' \quad (2b)$$

Empirical (discrete) correlation function $\rho_e(r)$ can be applied to approximate a distance r_o such that $\rho_e(r_o) \approx 0$. In terms of both exponential functions $\rho(r)$, this could be assumed as $\rho(r) \cong 0.05$. If so, then $r_o = \sqrt{3}d$ and $r_o = 3d'$; thus, $d \sim \sqrt{3}d'$. In this way, the following working hypothesis is derived: $\delta \sim 1.5\delta'$. A wider statistical analysis of the distance r_o and its confidence limits were presented by Jaksa et al. (1999). For $d >> 0$, the model turns to a degenerate spatial random field – just a random variable; for $d \sim 0$, the model

turns to a very chaotic random field with uncorrelated succeeding values.

There exist several sophisticated methods of evaluation of the δ-value; selected techniques and numerical results were presented by Bagińska et al. (2016), Lloret-Cabot et al. (2014), Pieczyńska-Kozłowska et al. (2017), Phoon and Kulhawy (1999a) and Vanmarcke (2010). Standard CPT testing is most often used – in vertical direction, first of all (Oguz et al. 2019); a very original horizontal CPT testing has been presented by Jaksa et al. (1999). Although the CPT method provides a very large amount of data – continuous realisations of the soil resistance, as expected for a stochastic process $q_c(z)$ – the interpretation of results encounters difficulties.

In the common opinion $\delta_h >> \delta_v$, like the ratio $\delta_h/\delta_v = 10$ used by Tietje et al. (2014); such proportion $\delta_h >> \delta_v$ can be suggested by a regular sedimentation of geological units. Again, for the same reasons as in cases of c.o.v., there is no agreed opinion about representative values of the scales of fluctuations δ. Moreover, in published data, the distinction between definitions in equations (2a) and (2b) is not always respected. For example, results of CPT soundings have been presented with the best fitted Gaussian curve (equation 1a) in the paper by Jaksa et al. (1999) – the authors report measured cone tip resistance q_c for which $\delta_v \sim 0.17$ m (average value) with a c.o.v. on the level of 30%. Independently, another value $r_o \cong 0.28$ m can be estimated from the authors' empirical plot of $\rho_e(r)$, used in place of the least-square fitting; in this way, the following values can be derived: $\delta_v = \sqrt{\pi} d_v = \sqrt{\pi} r_o/\sqrt{3} \cong r_o \cong 0.28$ m. Similar estimation $\delta_v \sim 0.8 \times 5.3/20 = 0.21$ m can be found from the same data using the Vanmarcke proposal $\delta_v \sim 0.8d$, where d denotes the average distance between intersections of the fluctuating resistance q_c and its parabolic trend function (Vanmarcke 2010, Jaksa et al. 1999). The horizontal scale of fluctuations δ_h was also analysed by Jaksa et al. (1999) and its nested structure was documented – the estimated results depend on the scale of sampling: $\delta_h \sim 0.15$ m for CPT sampling at 5 mm intervals (so, $\delta_h \cong \delta_v$), but $\delta_h \sim$ 1–2 m for CPT sampling at 0.5 and 1.0 m. The authors' conclusion says that 'both the small-scale vertical and lateral correlation distances are a manifestation of the CPT and not the soil itself' (Jaksa et al. 1999). On the other hand, the review by Phoon and Kulhawy (1999a) is in sharp contrast to the conclusions presented by Jaksa et al. (1999), but the former review is focused on a wider spectrum of testing methods, not only on the CPT sounding. For different geotechnical parameters, as well as for different testing techniques, there is generally $\delta_v \sim 1.0$–2.0 m (less than 1.0 m only for CPT tests), but δ_h is expressed in dozens of metres; so, the ratio $\delta_h/\delta_v \sim 10$ is confirmed. The references presented by Shen et al. (2021) for the offshore soil in the North Sea report $\delta_v \sim$ 0.48–7.14 m and $\delta_h \sim 24.62$–66.48 m.

3.1 Conclusion

For the illustrative numerical examples presented hereafter, the range of $d_v = \delta_v/\sqrt{\pi} \sim 0.5$–$1.5$ m and the range of $d_h = \delta_h/\sqrt{\pi} \sim 10$–$20$ m can be assumed as some representative values.

4 Prototype of the geometric spatial averaging

Standard spatial averaging, called as a geometric one, has a well-documented mathematical background presented by Vanmarcke (2010); also, it has many practical applications (Vanmarcke 2010, Chwała 2019, Tietje et al. 2011, Ching et al. 2016, Puła and Chwała 2015). For a frictional material, where $\tan(\varphi) > 0$ and $c = 0$ (kPa), consider two intervals dL extracted from a sliding line and assume the two random variables shown in Fig. 1a: a random variable $\tan(\varphi_1)$ on the left part dL and a random variable $\tan(\varphi_2)$ on the right one.

Looking for one 'effective' parameter, the random vector $(\tan(\varphi_1);\tan(\varphi_2))$ is replaced by one averaged random variable $\tan(\varphi)_{ga}$ acting along $2dL$. Assume the homogeneity condition: $E\{\tan(\varphi_i)\} = \mu$, $Var\{\tan(\varphi_i)\} = \sigma^2$; moreover, $Cov\{\tan(\varphi_1);\tan(\varphi_2)\} = \sigma^2 \times \rho_{1;2}$. The values dL are geometric weighting coefficients and the intuitively averaged (homogenised) friction coefficient $[\tan(\varphi)]_{ga}$ on $2dL$ can be calculated as a new random variable:

$$[\tan(\varphi)]_{ga} = [\tan(\varphi_1) \cdot dL + \tan(\varphi_2) \cdot dL]/(2dL) = \frac{1}{2} \cdot \tan(\varphi_1) + \frac{1}{2} \cdot \tan(\varphi_2) \quad (3)$$

Therefore, $E\{[\tan(\varphi)]_{ga}\} = \mu$, $Var\{[\tan(\varphi)]_{ga}\} = \sigma^2 \times (1 + \rho_{1;2})/2 < Var\{\tan(\varphi_i) = \sigma^2$. The variance reduction factor equals $\gamma_{ga} = Var\{[\tan(\varphi)]_{ga}\}/Var\{\tan(\varphi_i) = (1 + \rho_{1;2})/2 = 1 - (1 - \rho_{1;2})/2$; the lower index g refers to the purely geometric sense of equation (3). Note that potentially, the randomness of $[\tan(\varphi)]_{ga}$ in equation (3) can even disappear, if always both random fluctuations of $\tan(\varphi_1)$ and $\tan(\varphi_2)$ happen as opposite numbers, thus taking the hypothetic correlation coefficient $\rho_{1;2} = -1$.

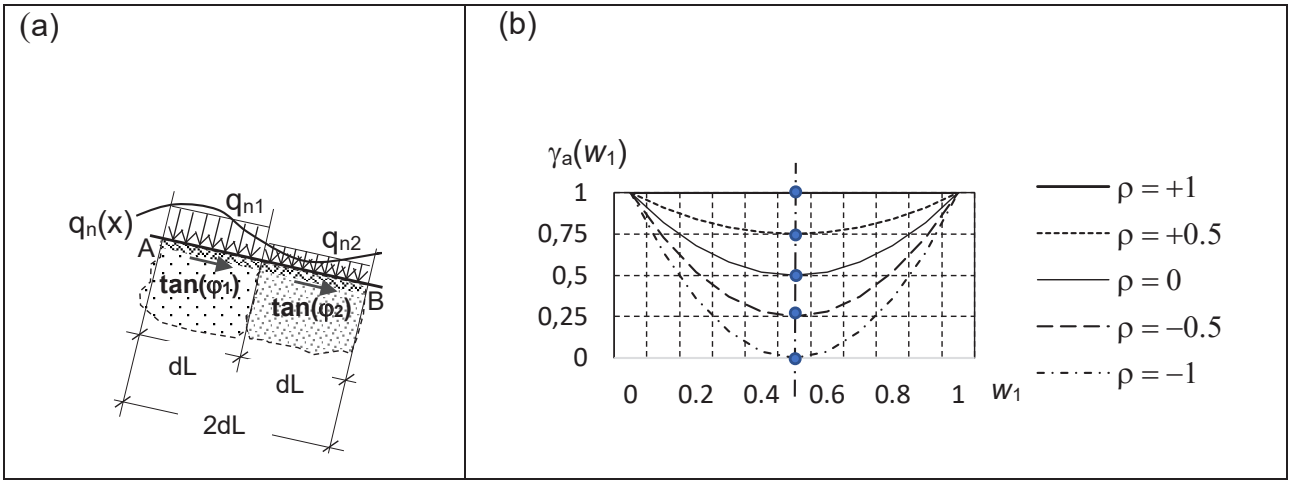

Figure 1: (a) Prototype defined by two random variables $\tan(\varphi_i)$, $i = 1, 2$. (b) Variance reduction factors $\gamma_a(w_1)$, depending on the dimensionless weight coefficient w_1.

Generalisations of the geometric averaging are straightforward, if for a longer interval AB, the sum in equation (3) is replaced by an integral over this line AB:

$$[\tan(\varphi)]_{ga} = \frac{\int_A^B \tan(\varphi(x))dx}{|AB|} = \frac{\int_A^B \tan(\varphi(x))dx}{\int_A^B 1dx} \quad (4)$$

where the interval length equals $|AB|$; the definition is similar for surfaces in spatial cases (Vanmarcke 2010).

5 Generalised methodology: prototype of the stress-weighted spatial averaging

Ultimate limit state for random shearing is a start point of this approach due to the context of the random vector $(\tan(\varphi_1);\tan(\varphi_2))$. For the frictional material, the two variables $\tan(\varphi_1)$, $\tan(\varphi_2)$ should be considered in conjunction with two normal deterministic loadings in Fig. 1a, $q_{n1} = \text{const} > 0$, $q_{n2} = \text{const} > 0$. The random shearing resistance along AB can be expressed as:

$$2dT = q_{n1} \cdot \tan(\varphi_1) \cdot dL + q_{n2} \cdot \tan(\varphi_2) \cdot dL \quad (5a)$$

Looking for one 'equivalent' random variable $[\tan(\varphi)]_{sa}$ on the same interval AB:

$$2dT = q_{n1} \cdot [\tan(\varphi)]_{sa} \cdot dL + q_{n2} \cdot [\tan(\varphi)]_{sa} \cdot dL = [\tan(\varphi)]_{sa} \cdot [q_{n1}+q_{n2}] \cdot dL \quad (5b)$$

Therefore, on comparing the two equations (5a) and (5b):

$$[\tan(\varphi)]_{sa} = \frac{q_{n1}\cdot\tan(\varphi_1)+q_{n2}\cdot\tan(\varphi_2)}{q_{n1}+q_{n2}} = w_1 \cdot \tan(\varphi_1) + w_2 \cdot \tan(\varphi_2) \quad (6)$$

where the dimensionless weight coefficients $w_i > 0$ equal $w_1 = q_{n1}/(q_{n1} + q_{n2})$, $w_2 = q_{n2}/(q_{n1} + q_{n2})$, $w_1 + w_2 = 1$.

In particular, the local contribution of $\tan(\varphi_1)$ is negligible if $q_{n1} << q_{n2}$, $w_1 << w_2$, so the randomness is localised, almost not averaged. If a (potentially possible) physical dependence between q_n and $\tan(\varphi)$ is ignored, then $E\{[\tan(\varphi)]_{sa}\} = w_1 \times \mu + w_2 \times \mu = \mu$ and $Var\{[\tan(\varphi)]_{sa}\} = [1 - 2 \times w_1 \times w_2 \times (1 - \rho_{1;2})] \times \sigma^2$.

Therefore, the variance reduction factor equals $\gamma_{sa} = Var\{[\tan(\varphi)]_{sa}\}/\sigma^2 = 1 - 2 \times w_1 \times (1 - w_1) \times (1 - \rho_{1;2})$; the lower index s refers to the stress-weighted averaging. The variance reduction factor γ_{sa} defined above is sensitive to q_n gradients and depends on the ratio q_{n1}/q_{n2}, what is not true for the variance reduction factor $\gamma_{ga} = 1 - (1 - \rho_{1;2})/2$, which is stress-independent. The following inequality $\gamma_{ga} \leq \gamma_{sa}$ is true, but $\gamma_{ga} = \gamma_{sa}$ if and only if $w_1 = w_2 = 1/2$, like for five dots depicted in Fig. 1b. To conclude, the geometric averaging has only an intuitive character, weakly related to the shearing resistance of frictional materials; the

overestimation of the beneficial variance reduction $\gamma_{ga} \leq \gamma_{sa}$ can be dangerous in safety evaluation. Parabolic functions $\gamma_{sa}(w_1)$ are depicted in Fig. 1b for five different correlation coefficients $\rho = \rho_{1;2}$.

Passage to a discrete multiterm sum for $n > 2$ random variables is straightforward; the same applies for a second-order stochastic process $\tan(\varphi(x))$ with an autocorrelation function $\rho(x;y)$ along the interval AB, where $E\{\tan(\varphi(x))\} = \mu = \text{const}$, $Var\{\tan(\varphi(x)\} = \sigma^2 = \text{const}$. The shearing resistance T is a random variable generated by the stationary stochastic process $\tan(\varphi(x))$ in the formula:

$$T = \int_A^B q_n(x) \cdot \tan(\varphi(x))\, dx \tag{7a}$$

Looking for an equivalent simplified model, the stochastic process $\tan(\varphi(x))$ is replaced by a random variable $[\tan(\varphi)]_{sa} = \text{const}(x)$. If so, the same random variable T has the following form:

$$T = \int_A^B [\tan(\varphi)]_{sa} \cdot q_n(x) dx = [\tan(\varphi)]_{sa} \cdot \int_A^B q_n(x) dx \tag{7b}$$

Both alternative expressions for the same random variable T formulate the background for the definition of $[\tan(\varphi)]_{sa}$; if equations (7a) and (7b) are compared, the following definition can be obtained:

$$[\tan(\varphi)]_{sa} = \frac{\int_A^B q_n(x) \cdot \tan(\varphi(x)) dx}{\int_A^B q_n(x) dx} \tag{8}$$

Therefore,

$$E\{[\tan(\varphi)]_{sa}\} = \frac{\int_A^B q_n(x) \cdot E\{\tan(\varphi(x))\} dx}{\int_A^B q_n(x) dx} = \frac{\int_A^B q_n(x) \cdot \mu\, dx}{\int_A^B q_n(x) dx} = \mu \tag{9a}$$

$$Var\{[\tan(\varphi)]_{sa}\} = \frac{\int_A^B \int_A^B q_n(x) \cdot q_n(y) \cdot Cov\{\tan(\varphi(x)); \tan(\varphi(y))\} dx dy}{\left[\int_A^B q_n(x) dx\right]^2} \tag{9b}$$

The dimensionless variance reduction factor equals

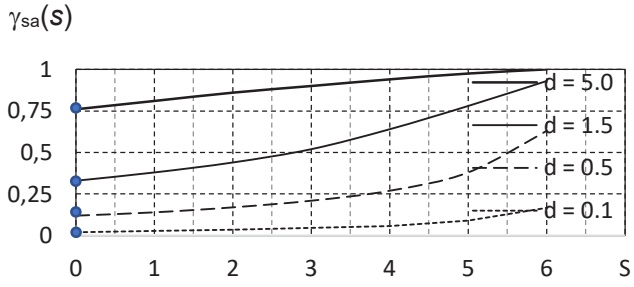

Figure 2: The dimensionless variance reduction factors $\gamma_{sa}(S)$ depending on the correlation parameter d (m) and the stress parameter S (m).

$$\gamma_{sa} = \frac{Var\{[\tan(\varphi)]_{sa}\}}{Var\{\tan(\varphi(x))\}} = \frac{Var\{[\tan(\varphi)]_{sa}\}}{\sigma^2} = \frac{\int_A^B \int_A^B q_n(x) \cdot q_n(y) \cdot \rho(x;y) dx dy}{\left[\int_A^B q_n(x) dx\right]^2} \leq 1 \tag{10}$$

where $\rho(x;y) = \rho(x - y)$ because of the assumed homogeneity; the expression (10) has only loose ties with the approximate variance reduction factor proposed for practical applications by Vanmarcke (2010): $\Gamma^2 = \min\{1; \delta/|AB|\}$.

Only if $q_n = \text{const}$ along AB, then the geometric averaging coincides with stress-weighted averaging, but generally the latter one is more representative.

Simple numerical results are presented in Fig. 2; a fixed interval AB of length $|AB|$=7 m is loaded in a localised way on [0;7]: $q_n(x) = 0$ on [0;S], $0 \leq S < 7$, and $q_n(x) = q = \text{const} > 0$ on (S;7], so in the Heaviside form, $q_n(x) = q \times [H(x - S) - H(x - 7)]$; the Gaussian autocorrelation $\rho(x;y) = \exp\{-[(x-y)/d]^2\}$, $0 \leq x, y \leq 7$ is assumed. Both methods coincide if and only if $S = 0$ (four dots on the vertical axis), but $\gamma_{ga} < \gamma_{sa}$ elsewhere; the geometric spatial averaging is insensitive to the length S, which describes very different stresses along AB.

6 Example: resistance against horizontal sliding

As a practical example, consider the standard GEO-sliding stability condition (EN 1997-1) for a massive shallow foundation $BxLxh$, where $-B/2 \leq x_1 \leq +B/2$ and $-L/2 \leq x_2 \leq +L/2$. Define normal (vertical) contact stresses under the footing as $q_n(x_1,x_2) = q_n(\underline{x}) \geq 0$. The foundation base BxL is horizontal and 'rough', that is, the stabilising horizontal

force can be calculated from the simple frictional model as $T = V \times \tan(\varphi)$, if the subsoil is cohesionless; note that this deterministic model does not depend on the eccentricities of the deterministic vertical load V called as e_B and e_L, respectively.

In the random variable format, the friction coefficient $\tan(\varphi)$ in the expression $T = V \times \tan(\varphi)$ has a mean value μ and a variance σ^2, so $E\{T\} = V\mu$, $Var\{T\} = V^2\sigma^2$. For a second-order homogeneous isotropic random field $\tan(\varphi(x_1,x_2)) = \tan(\varphi(\underline{x}))$ and the random shearing resistance, T can be expressed following equations (7a) and (7b), that is:

$$T = \int_{BxL} q_n(\underline{x}) \cdot \tan\left(\varphi(\underline{x})\right) d\underline{x} \text{ and,}$$
$$\text{on the other hand, } T = [\tan(\varphi)]_{sa} \cdot \int_{BxL} q_n(\underline{x})\, d\underline{x} \quad (11)$$

Therefore,

$$[\tan(\varphi)]_{sa} = \frac{\int_{BxL} q_n(\underline{x}) \cdot \tan\left(\varphi(\underline{x})\right) d\underline{x}}{\int_{BxL} q_n(\underline{x}) d\underline{x}} \text{ and eventually,}$$
$$\gamma_{sa} = \frac{\int_{BxL}\int_{BxL} q_n(\underline{x}) \cdot q_n(\underline{y}) \cdot \rho(\underline{x};\underline{y}) \cdot d\underline{x} d\underline{y}}{\left[\int_{BxL} q_n(\underline{x}) d\underline{x}\right]^2} \quad (12)$$

Note that the vertical coordinate x_3 (or simply z) is not used in this model.

The presented numerical example employs the horizontally isotropic Gaussian autocorrelation function $\rho(\underline{x};\underline{y}) = \exp\{-[(x_1 - y_1)/d_h]^2 - [(x_2 - y_2)/d_h]^2\}$; following the recommendations of the Eurocode 7 (EN 1997-1), the vertical contact stress q_n under the footing can be assumed as a double linear function like $q_n(\underline{x}) = a_o + a_1x_1 + a_2x_2$ (kPa). Consider a symmetrical case $B = L = 10$ m, V =10 MN, $q = V/(B \times L) = 100$ kPa, $e_B = e_L = e$ (m) ≥ 0.

If both eccentricities $0 \leq e < 10/12$ m, then under the corners: $q_1 = 100 + 120 \times e$, $q_2 = q_3 = 100$, $q_4 = 100 - 120 \times e > 0$, so $q_n(\underline{x}) = 100 + 12 \times e \times (x_1 + x_2)$ (kPa).

If both eccentricities $e > 10/12$, then a gap appears under foundation (zero contact stress, locally); for a maximal value e = 30/12 m, which is the maximal acceptable by the Eurocode 7, there is $q_n(\underline{x}) = \max\{0;60 \times (x_1 + x_2)\}$ (kPa).

The values of the variance reduction factor γ_{sa} are depicted in Fig. 3 for $e \leq 30/12$ m.

The geometric spatial averaging and the variance reduction factor γ_{ga} do not depend on the eccentricities e and they overestimate the variance reduction effects (four dots in Fig. 3). Special attention should be paid to the curves for $d \sim 20$ m and $d \sim 10$ m, which correspond to the most realistic values of the horizontal correlation parameter d_h:

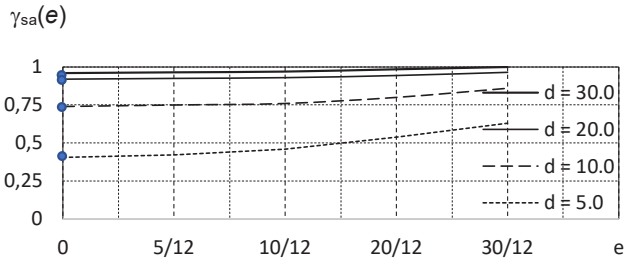

Figure 3: The dimensionless variance reduction factors $\gamma_{sa}(e)$ depending on the correlation parameter $d = d_h$ (m) and the load eccentricities $e_B = e_L = e$ (m).

- for d_h = 10 m, the variance reduction γ_{sa} is on the level of 74%–87%, whereas γ_{ga} = 74%;
- for d_h = 20 m, the variance reduction γ_{sa} is only on the level of 92%–97%, whereas γ_{ga} = 92% and
- for d_h = 30 m, the variance reduction γ_{sa} is only on the level of 96%–99%, whereas γ_{ga} = 96%.

6.1 Conclusion

The results are close to each other and for $d_h \geq 20$ m, both horizontal variance reductions are not significant; still much greater L or B (for dams, weirs, etc.) would be necessary to observe greater reduction. Both spatial averaging methods do not seem to be necessary for such proportions of the object dimensions B, L and d_h, that is, if $d_h/L > 2$–3.

7 Example: settlement analysis of a shallow foundation

The integral equations (7)–(10) apply not only to shearing resistance, but also to settlement analysis and to any linear operator, in fact. In a simplified linear form suggested by the Eurocode 7 (EN 1997-1), the foundation settlement w (m) can be estimated as follows:

$$w = \int_0^{z_{max}} q_n(z) \cdot D(z) dz \quad (13a)$$

The symbol $D(z) > 0$ (1/kPa) denotes a random deformation modulus – stationary stochastic process as a function of the depth $x_3 = z > 0$ under foundation.

The following equivalent $[D]_{sa}$ = const(z) as a corresponding random variable can be introduced:

$$w = \int_0^{z_{\max}} [D]_{\mathrm{sa}} \cdot q_n(z)dz = [D]_{\mathrm{sa}} \cdot \int_0^{z_{\max}} q_n(z)dz \quad (13b)$$

Equations (13a) and (13b) define the random variable $[D]_{sa}$.

Equations (13a) and (13b) are focused on a finite interval $0 \le z \le z_{max}$ under a shallow footing; taking into account a founding depth h_f under the ground surface, the value of z_{max} can be estimated from the equation $\gamma\times(h_f/B + z_{max}/B)\times B\times 0.2 = q_n(z_{max})$ (EN 1997-1), where $\gamma\times(h_f + z)$ denotes vertical stresses *in situ* for a dry soil and γ (kN/m^3) is the subsoil unit weight. The average vertical stress q_n under a rectangular footing *BxL* vanishes with depth *z*; usually, the integrated Steinbrenner formula is in use (a double integral of the Boussinesq solution) or just the following simplified estimation: $q_n(z) = V/[(B + z)\times(L + z)] = q/[(1 + z/B)\times(1 + \beta\times z/B)]$ for $\beta = B/L \le 1$, $q = V/(B\times L) = \mathrm{const} > 0$. The deterministic depth z_{max} depends on the β coefficient as in Fig. 4. It is assumed that random fluctuations of $D(z)$ do not change the deterministic load function $q_n(z)$ and vice versa.

The stochastic parameter $D(z)$ (1/kPa) needs a comment. Clearly, the random deformation modulus $D(z)$ corresponds to $1/E(z)$ or $1/M(z)$ by making use of the Young modulus E or the oedometric modulus M of the subsoil; both are assumed as stochastic processes. As far as distribution-free models are considered, the first two moments $E\{D(z)\} = \mu = \mathrm{const}(z)$, $Var\{D(z)\} = \sigma^2 = \mathrm{const}(z)$, $Cov\{D(z_1);D(z_2)\} = \sigma^2\times\rho(z_1 - z_2)$ cannot be derived from the corresponding moments $E\{M(z)\}$, $Cov\{M(z_1);M(z_2)\}$ – the model should be completed by some joint probability distributions of the stochastic process $M(z)$; in particular, correlated lognormal random variables $M(z_1)$, $M(z_2)$ can be useful. Alternatively, the first-order perturbation is acceptable for a 'small' variance of $M(z)$; also, an adequate data pre-processing can be recommended to apply the sample statistics directly to $1/M$, not to M, because the stationarity of both $1/M$ and M has different conditions.

Equations (13a) and (13b) yield the variance of the averaged deformation modulus $Var\{[D]_{sa}\}$ and then the variance reduction factor equals:

$$\gamma_{\mathrm{sa}} = \frac{Var\{[D]_{\mathrm{sa}}\}}{Var\{D(z)\}} = \frac{\int_0^{z_{\max}}\int_0^{z_{\max}} q_n(z_1)\cdot q_n(z_2)\cdot\rho(z_1;z_2)dz_1dz_2}{\left[\int_0^{z_{\max}} q_n(z)dz\right]^2} \le 1 \quad (14)$$

Spatial horizontal random fluctuations are much less significant for such rectangular footing *BxL*; they are not considered here ($d_h >> d_v$).

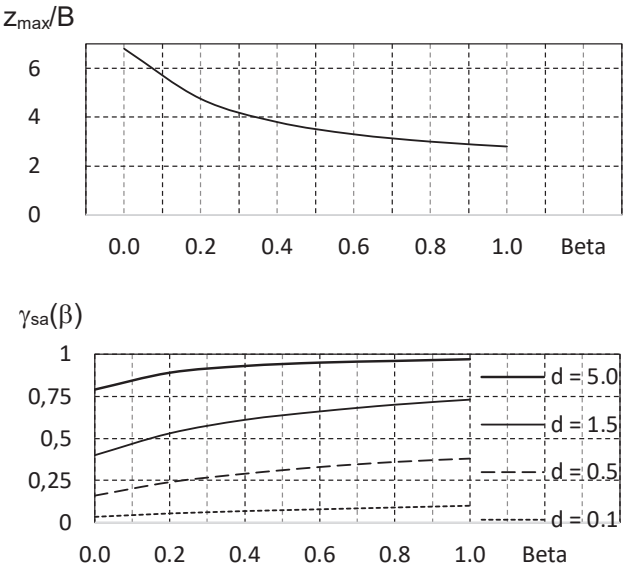

Figure 4: The effective depth z_{max} under considered foundation and the dimensionless variance reduction factor $\gamma_{sa}(\beta)$ depending on the correlation parameter $d = d_v$(m) and the footing shape ratio β.

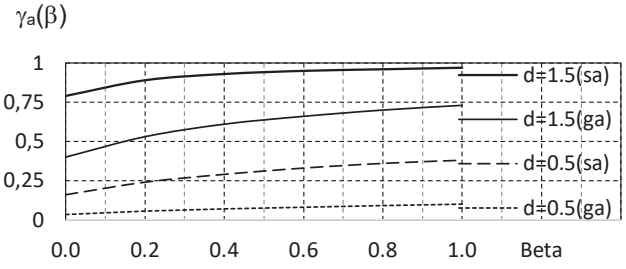

Figure 5: The dimensionless variance reduction factors $\gamma_{sa}(\beta)$ and $\gamma_{ga}(\beta)$ for the correlation parameters $d_v = d = 1.5$ m (solid lines) and $d_v = d = 0.5$ m (dashed lines).

The numerical example in Fig. 4 uses the Gaussian autocorrelation function $\rho(z_1;z_2) = \exp\{-[(z_1 - z_2)/d_v]^2\}$, $0 \le z_1, z_2 \le z_{max}$; the subsoil unit weight $\gamma = 18$ kN/m^3, $q = 250$ kPa, $h_f/B = 2$ and the foundation width $B = 1$ m. For such fixed data, the effective dimensionless z_{max}/B depends on the dimensionless shape coefficient $\beta = B/L \le 1$ as in Fig. 4; the shape ratio $\beta = 0$ corresponds to an infinite beam and $\beta = 1$ corresponds to a square footing.

The geometric variance reduction factor γ_{ga} in Fig. 5 is also derived from equation (14) for the same z_{max}, but for $q_n = \mathrm{const}(z)$. Differences between the factors γ_{sa} and γ_{ga} in Fig. 5 are significant.

8 Cohesive soils

For perfectly cohesive materials, the shearing resistance in Fig. 1a equals $2dT = c_1 \times dL + c_2 \times dL$ and is replaced by $2dT = [c]_a \times dL + [c]_a \times dL$; hence, $[c]_a = (c_1 + c_2)/2$. For such a case, the geometric spatial averaging (Vanmarcke 2010) is representative because the model is independent of the normal stress $q_n > 0$. There is only one averaged cohesion:

$$[c]_a = [c]_{sa} = [c]_{ga} = \frac{\iint_D c(\underline{x})d\underline{x}}{\iint_D 1 d\underline{x}} \tag{15}$$

and only one dimensionless reduction coefficient $\gamma_a = \gamma_{sa} = \gamma_{ga}$.

To be precise, there exist some rare exceptions because this is not the soil cohesion (or adhesion) itself which generates the shearing resistance, but the soil cohesion (or adhesion) on a real contact with the foundation. As in section 6, a gap can appear under a rigid foundation for 'great' eccentricities e, hence the averaging is limited (localised) only to a soil–foundation direct contact ($q_n > 0$); to a certain extent, for a rigid foundation, the model is not completely independent of q_n, so γ_{ga} can be less than γ_{sa} also for perfectly cohesive soils. This aspect is not analysed below.

Although the Tresca model with $\tan(\varphi) \equiv 0$, $c > 0$ found certain practical applications to undrained bearing capacity, this is, however, a peculiar case. Generally, the shearing ultimate limit states are stress dependent, not only for the Coulomb material. In a general case of $\tau(\underline{x}) = q_n(\underline{x}) \times \tan(\varphi(\underline{x})) + c(\underline{x})$, two homogeneous random fields are considered for a frictional–cohesive soil. Both autocovariance functions are completed by a crosscovariance function $Cov\{\tan(\varphi(\underline{x})); c(\underline{y})\} = \sigma_{\tan(\varphi)} \times \sigma_c \times r_{\tan(\varphi);c} \times \rho_{\tan(\varphi);c}(\underline{x} - \underline{y})$. More or less significant distinctions between the decay functions $\rho_{\tan(\varphi)}(\underline{x} - \underline{y})$, $\rho_c(\underline{x} - \underline{y})$ and $\rho_{\tan(\varphi);c}(\underline{x} - \underline{y})$ are possible. If $q_n(\underline{x}) > 0$, then the usual definition of a local shear coefficient $\tan(\psi(\underline{x})) = \tan(\varphi(\underline{x})) + c(\underline{x})/q_n(\underline{x}) > \tan(\varphi(\underline{x}))$ reduces the situation to an equivalent cohesionless material. The new random field $\tan(\psi(\underline{x}))$ is not homogeneous if $q_n(\underline{x}) \neq \text{const}(\underline{x})$; in particular, $E\{\tan(\psi(\underline{x}))\} = \mu_{\tan(j)} + \mu_c/q_n(\underline{x})$, $Var\{\tan(\psi(\underline{x}))\} \neq \text{const}(\underline{x})$. By making use of the procedure defined by equations (7) and (8) for the frictional soil,

$$T\left(\tan\left(\varphi(\underline{x})\right); c(\underline{x})\right) = \iint_D q_n(\underline{x}) \cdot \tan\left(\psi(\underline{x})\right) d\underline{x} \tag{16a}$$

$$T([\tan(\psi)]_{sa}) = \iint_D [\tan(\psi)]_{sa} \cdot q_n(\underline{x})\, d\underline{x} = [\tan(\psi)]_{sa} \cdot \iint_D q_n(\underline{x})\, d\underline{x} \tag{16b}$$

Therefore,

$$[\tan(\psi)]_{sa} = \frac{\iint_D q_n(\underline{x}) \cdot \tan\left(\varphi(\underline{x})\right) d\underline{x} + \iint_D c(\underline{x}) d\underline{x}}{\iint_D q_n(\underline{x}) d\underline{x}} = [\tan(\varphi)]_{sa} + [c]_a \cdot \frac{\iint_D 1 d\underline{x}}{\iint_D q_n(\underline{x}) d\underline{x}} \tag{17}$$

Here, the variance reduction factor (equation 10) is less useful because it is a position-dependent function (in the denominator):

$$\gamma_{sa} = \frac{Var\{[\tan(\psi)]_{sa}\}}{Var\left\{\tan\left(\psi(\underline{x})\right)\right\}},\ \underline{x} \in D \tag{18}$$

Alternatively, the vectorial random field $(\tan(\varphi(\underline{x})); c(\underline{x}))$ can be replaced by the equivalent random vector $([\tan(\varphi)]_{sa}; [c]_a)$ by making use of the previously defined averages. Depending on a stress level of $q_n(\underline{x})$ – not only on gradients – either the value $[\tan(\varphi)]_{sa}$ or $[c]_a$ dominates in the averaging; thus, the interpretation becomes more complex. To overcome this difficulty, the effect of the variance reduction can be studied in terms of the random shearing resistance T, not in terms of its strength parameters. Therefore,

$$\gamma_{sa} = \frac{Var\{T([\tan(\varphi)]_{sa}; [c]_a)\}}{Var\{T(\tan(\varphi); c)\}} = \frac{Var\left\{[\tan(\varphi)]_{sa} \cdot \iint_D q_n(\underline{x}) d\underline{x} + [c]_a \cdot \iint_D 1 d\underline{x}\right\}}{Var\left\{\tan(\varphi) \cdot \iint_D q_n(\underline{x}) d\underline{x} + c \cdot \iint_D 1 d\underline{x}\right\}} \tag{19}$$

The random solution $T(\tan(\varphi); c)$ in the denominator operates simply on the (correlated) random variables $\tan(\varphi)$, c, yielding from the random fields $\tan(\varphi(\underline{x}))$, $c(\underline{x})$ when ignoring their spatial effects, that is, for $\rho(\underline{x}; \underline{y}) \equiv 1$.

9 Example: wedge stability

9.1 Data analysis

A simple discretised random field which corresponds to Fig. 1a is depicted in Fig. 6. For a potential sliding mechanism in 2D, four crosscorrelated random variables are considered: $X_1 = \tan(\varphi_1)$, $X_2 = \tan(\varphi_2)$, $X_3 = c_1$, $X_4 = c_2$; the sliding wedge is split into two homogeneous triangles ADB and DCB.

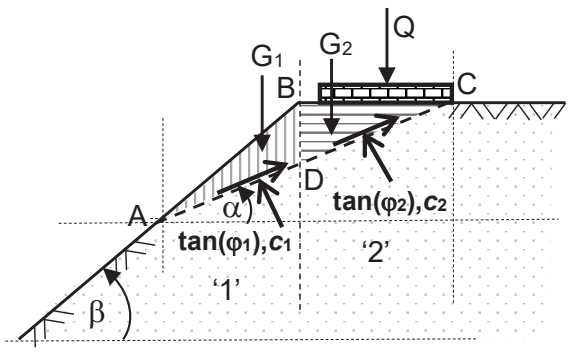

The design situation is as follows:
For the slope $\beta = 41^o$
For the wedge $\alpha = 24^o$
BC = 4.0 m
AD = L_1 = 4.6 m, DC = L_2 = 4.4 m
Unit weight $\gamma = 18$ kN/m^3
G_1 = 67 kN/m, G_2 = 64 kN/m
Q = 3.5 m·60 kPa = 210 kN/m

Figure 6: Simplified wedge stability for 2*x*2 random variables $\tan(\varphi_i)$, c_i, $i = 1, 2$.

Table 1: Auto- and cross-covariances used in numerical calculations.

$Cov\{X_i;X_j\}$	$\tan(\varphi_1)$ (-)	$\tan(\varphi_2)$ (-)	c_1 (kPa)	c_2 (kPa)
$\tan(\varphi_1)$ (-)	0.015625	0.0015625	−0.15	−0.03
$\tan(\varphi_2)$ (-)	0.0015625	0.015625	−0.03	−0.15
c_1 (kPa)	−0.15	−0.03	16	1.6
c_2 (kPa)	−0.03	−0.15	1.6	16

Table 2: Auto- and crosscorrelation coefficients used in numerical calculations.

ρ_{ij}	$\tan(\varphi_1)$	$\tan(\varphi_2)$	c_1	c_2
$\tan(\varphi_1)$	1	+0.10	−0.30	−0.06
$\tan(\varphi_2)$	+0.10	1	−0.06	−0.30
c_1	−0.30	−0.06	1	+0.10
c_2	−0.06	−0.30	+0.10	1

The randomly inhomogeneous material corresponds to a silty–clayey sand. The second-order moments are assumed as follows: $E\{\tan(\varphi_i)\} = 0.5$, $\sigma_{\tan(\varphi i)} = 0.125$, $\nu_{\tan(\varphi i)} = 25\%$, $E\{c_i\} = 10.0$ kPa, $\sigma_{ci} = 4.0$ kPa, $\nu_{ci} = 40\%$. The covariance matrix is presented in Table 1, and dimensionless correlation coefficients are depicted in Table 2.

The second-order moments of the random variables $\tan(\varphi_i)$, c_i are assumed as the discrete input data; if they are discretised from the continuous spatial moments, like $Cov\{\tan(\varphi(\underline{x}));c(\underline{y})\}$ in the random field formulation, then they are 'close' to mid-point values on *AD*, *DC*, but are not exactly the same – particularly, if the distinguished macro-homogeneous regions are not 'small'. This aspect is not considered here.

9.2 Results of the presented parameter-averaging procedures

The obtained averaged values of the friction coefficients are as follows:

$$[\tan(\varphi)]_{ga} = [\tan(\varphi_1)\times L_1 + \tan(\varphi_2)\times L_2]/(L_1 + L_2) = 0.511\times\tan(\varphi_1) + 0.489\times\tan(\varphi_2)$$
$$Var\{[\tan(\varphi)]_{ga}\} = 0.00860 = 0.550\times 0.125^2,$$
$$\gamma_{ga} = Var\{[\tan(\varphi)]_{ga}\}/Var\{\tan(\varphi)\} = 0.55$$
$$[\tan(\varphi)]_{sa} = [\tan(\varphi_1)\times G_1 + \tan(\varphi_2)\times(G_2 + Q)]\times\cos(\alpha)/[(G_1 + G_2 + Q)\times\cos(\alpha)] = 0.196\times\tan(\varphi_1) + 0.804\times\tan(\varphi_2)$$
$$Var\{[\tan(\varphi)]_{sa}\} = 0.0112 = 0.716\times 0.125^2,$$
$$\gamma_{sa} = Var\{[\tan(\varphi)]_{sa}\}/Var\{\tan(\varphi)\} = 0.72 > 0.55.$$

Moreover,

$$[c]_a = [c]_{ga} = [c]_{sa} = (c_1\times L_1 + c_2\times L_2)/(L_1 + L_2) = 0.511\times c_1 + 0.489\times c_2,$$
$$Var\{[c]_a\} = 8.803 = 0.550\times 4.0^2,\ \gamma_a = \gamma_{ga} = \gamma_{sa} = Var\{[c]_a\}/Var\{c\} = 0.55.$$

New 'macro' correlation coefficients are negative and they equal:
−0.33 between the random variable $[\tan(\varphi)]_{ga}$ and the random variable $[c]_a$ and
−0.28 between the random variable $[\tan(\varphi)]_{sa}$ and the random variable $[c]_a$.

$Var\{T([\tan(\varphi)]_{ga};[c]_{ga}\} = 1040$, $Var\{T([\tan(\varphi)]_{sa};[c]_{sa}\} = 1310$, $Var\{T(\tan(\varphi;c\} = 1975$; therefore, the definition in equation (19) results in $\gamma_{sa} = 1310/1975 = 0.66 > \gamma_{ga} = 1040/1975 = 0.53$.

9.3 Random factors of safety

Since the wedge stability is analysed, the randomness of the factor of safety (*FS*) requires a further numerical study. The standard *FS* is defined using the stabilising frictional–cohesive force T_{stab} and the destabilising shearing one T_{dst}:

$$FS = \frac{T_{stab}}{T_{dst}} = \frac{G_1 \cdot \cos(\alpha) \cdot \tan(\varphi_1) + (G_2 + Q) \cdot \cos(\alpha) \cdot \tan(\varphi_2) + L_1 \cdot c_1 + L_2 \cdot c_2}{G_1 \cdot \sin(\alpha) + (G_2 + Q) \cdot \sin(\alpha)} \quad (20a)$$

By analogy, the dimensionless variance reduction factors are expressed as a fraction of $Var\{FS(\tan(\varphi);c)\}$, where $FS(\tan(\varphi);c)$ is calculated using the point variances of the random field, that is, $\sigma_{\tan(\varphi)} = 0.125$ and $\sigma_c = 4.0$ kPa.

1) Reference case No. 1: the model of two random variables, not averaged.

Ignoring the spatial randomness, as in the denominator of equation (19), so for the model of two correlated random variables $\tan(\varphi_1) = \tan(\varphi_2) = \tan(\varphi)$ and $c_1 = c_2 = c$ (no spatial decay function, $\rho \equiv 1$), equation (20a) becomes:

$$FS = \frac{T_{stab}}{T_{dst}} = \frac{[G_1 \cdot \cos(\alpha) + (G_2 + Q) \cdot \cos(\alpha)] \cdot \tan(\varphi) + (L_1 + L_2) \cdot c}{G_1 \cdot \sin(\alpha) + (G_2 + Q) \cdot \sin(\alpha)} = \frac{\tan(\varphi)}{\tan(\alpha)} + \frac{(L_1 + L_2) \cdot c}{G_1 \cdot \sin(\alpha) + (G_2 + Q) \cdot \sin(\alpha)} \quad (20b)$$

In the considered case $FS = FS(\tan(\varphi);c) = 2.25 \times \tan(\varphi) + 0.0649 \times c$; so, $E\{FS(\tan(\varphi);c)\} = 1.77$ and $Var\{FS(\tan(\varphi);c)\} = 0.1030$.

2) Reference case No. 2: the exact model with two random fields (two random vectors in discretisation, that is, four random variables), not averaged (Fig. 6).

The explicit equation (20a) is used which has the following form:

$FS = FS(\tan(\varphi_1),\tan(\varphi_2);c_1,c_2) = 0.441 \times \tan(\varphi_1) + 1.80 \times \tan(\varphi_2) + 0.0332 \times c_1 + 0.0317 \times c_2$; so, $E\{FS(\tan(\varphi_1),\tan(\varphi_2);c_1,c_2)\} = 1.77$ and $Var\{FS(\tan(\varphi_1),\tan(\varphi_2);c_1,c_2)\} = 0.0673$.

The exact variance reduction factor $\gamma_{FS} = 0.0673/0.1030 = 0.65$.

3) The simplified model of geometrical averaging $[.]_{ga}$: reduction from two random fields (two random vectors) to two random variables.

Using the geometrical averaging, thus the random variable $[\tan(\varphi)]_{ga}$ which is calculated along AD, DC in section 9.2:

$$FS = \frac{T_{stab}}{T_{dst}} = \frac{G_1 \cdot \cos(\alpha) \cdot [\tan(\varphi)]_{ga} + (G_2 + Q) \cdot \cos(\alpha) \cdot [\tan(\varphi)]_{ga} + (L_1 + L_2) \cdot [c]_{ga}}{G_1 \cdot \sin(\alpha) + (G_2 + Q) \cdot \sin(\alpha)} \quad (20c)$$

where $[c]_{ga} = [c]_a = (L_1 \times c_1 + L_2 \times c_2)/(L_1 + L_2)$.

In the considered case, $FS = FS([\tan(\varphi)]_{ga};[c]_{ga}) = 1.15 \times \tan(\varphi_1) + 1.10 \times \tan(\varphi_2) + 0.0332 \times c_1 + 0.0317 \times c_2$; so, $E\{FS([\tan(\varphi)]_{ga};[c]_{ga})\} = 1.77$ and $Var\{FS([\tan(\varphi)]_{ga};[c]_{ga})\} = 0.0543$.

The calculated variance reduction factor $\gamma_{FS} = 0.0543/0.1030 = 0.53$ underestimates the exact result $\gamma_{FS} = 0.65$.

4) The simplified model of stress-weighted averaging $[.]_{sa}$: reduction from two random fields (two random vectors) to two random variables.

Using the stress-weighted averaging, thus the random variable $[\tan(\varphi)]_{sa}$ which is calculated along AD, DC in section 9.2:

$$FS = \frac{T_{stab}}{T_{dst}} = \frac{G_1 \cdot \cos(\alpha) \cdot [\tan(\varphi)]_{sa} + (G_2 + Q) \cdot \cos(\alpha) \cdot [\tan(\varphi)]_{sa} + (L_1 + L_2) \cdot [c]_{sa}}{G_1 \cdot \sin(\alpha) + (G_2 + Q) \cdot \sin(\alpha)} \quad (20d)$$

where $[c]_{sa} = [c]_a = (L_1 \times c_1 + L_2 \times c_2)/(L_1 + L_2)$.

In the considered case, $FS = FS([\tan(\varphi)]_{sa};[c]_{sa}) = 0.441 \times \tan(\varphi_1) + 1.80 \times \tan(\varphi_2) + 0.0332 \times c_1 + 0.0317 \times c_2$; so, $E\{FS([\tan(\varphi)]_{sa};[c]_{sa})\} = 1.77$ and $Var\{FS([\tan(\varphi)]_{sa};[c]_{sa})\} = 0.0673$.

The obtained variance reduction factor $\gamma_{FS} = 0.0673/0.1030 = 0.65$ confirms the exact solution from previous reference case No. 2. No probabilistic information is lost during the stress-weighted averaging.

All the approaches are unbiased, that is, $E\{FS\} = 1.77 = \text{const}$; the presented results reveal that the model of two random variables (ignoring spatial variability) overestimates the exact variance of 53% (0.103/0.0673 = 1.53), the $[.]_{ga}$ model underestimates the exact variance of 20% (0.0543/0.0673 = 0.80) and the $[.]_{sa}$ model is exact (0.0673/0.0673 = 1). For weakly correlated random fields, especially for non-cohesive materials, the differences are more significant.

Note that for *n* discrete elements, $n > 2$, and for local angles $\alpha_1, \ldots, \alpha_n$, the presented example of the wedge stability has a direct generalisation to the method of slices by Fellenius or Bishop.

10 Summary and conclusions

1) There exist three basic sources of subsoil randomness: the inherent randomness *in situ* (including meso- or macro-inhomogeneity trends), measurement errors and possible (mis)interpretations or data transformation uncertainty; the paper focuses on a fourth factor – the field of stresses in a subsoil, which can amplify (or suppress) some spatial random fluctuations of subsoil parameters.
2) The basic statistical measures of subsoil parameters' variability, that is, the coefficient of variation, auto- and crosscorrelation lengths (scales of fluctuations δ), are reported in numerous papers, but the results are often divergent; this is caused by mostly unknown geological processes (sedimentation, overloading, 3D consolidation, weathering), different particle morphology, water content, soil testing methodology, etc. Generally, there is a wide margin of uncertainty and only some trends or provisional intervals can be concluded from literature studies – until a local programme of subsoil investigations is implemented.
3) For practical reasons, in the context of simple design situations, it is recommended to replace the vectorial random field $(\tan(\varphi(\underline{x}));c(\underline{x}))$ by an equivalent random vector consisting of spatially averaged values $([\tan(\varphi)]_a;[c]_a)$.
4) If the strength parameters of the Coulomb material can be analysed as homogeneous random fields $(\tan(\varphi(\underline{x}));c(\underline{x}))$, then the spatial auto- and cross-correlations $\rho < 1$ reduce the variance of the random shearing resistance T due to interactions between adjacent regions; the reduction effects are significant if the scale of fluctuations δ (m) is short – in vertical direction most frequently.
5) As far as frictional materials are considered, the method of averaging proposed by E. Vanmarcke is controversial because it has no formalised background and the volume averaging is not representative; it overestimates the variance reduction effects, and hence, it overestimates the structural safety and can be dangerous in risk assessment. The same can be concluded for settlements and serviceability limit states.
6) The paper presents a rational alternative defined as the stress-weighted averaging, which is a more general approach; only for perfectly cohesive soils or uniform loadings, both methods coincide.
7) Several simple examples illustrate the proposed averaging procedures and reveal that the averaging is problem dependent; moreover, even for the same design situation, like in the example of wedge stability, the analyses are sensitive to basic deterministic parameters (sliding angle α and others).
8) The conclusions are true for a much wider class of design situations; for example, the standard Fellenius-type slope stability analysis is a straightforward multidimensional generalisation of the presented numerical example (wedge stability), using the stress-weighted averaging along cylindrical surfaces and local angles α_i.

References

[1] Bagińska, I., Kawa, M. & Janecki, W. (2016). Spatial variability of lignite mine dumping ground soil properties using CPTu results. *Studia Geotechnica et Mechanica, 38*(1), 3-13.

[2] Brząkała, W. (1981). Randomness of subsoil parameters (in Polish). *Archiwum Inżynierii Lądowej* (*Archives of Civil Engineering*), XXVII(4), 599-606.

[3] Ching, J. & Hu, Y.-G. (2017). Effective Young's modulus for a footing on a spatially variable soil mass. Geo-Risk 2017, ASCE Conf. Proceedings, Denver, USA, 360-369.

[4] Ching, J., Hu, Y.G. & Phoon, K.K. (2016). On characterizing spatially variable soil shear strength using spatial average. *Probabilistic Engineering Mechanics*, *45*, 31-43.

[5] Ching, J. & Phoon, K.K. (2013). Mobilized shear strength of spatially variable soils under simple stress states. *Structural Safety*, *41*, 20-28.

[6] Cho, S.E. (2007). Effects of spatial variability of soil properties on slope stability. *Engineering Geology*, *92*, 97–109.

[7] Chwała, M. (2019). Undrained bearing capacity of spatially random soil for rectangular footings. *Soils and Foundations, 59*(5), 1508-1521.

[8] Deng, Z.P., Li, D.Q., Qi, X.H., Cao, Z.J. & Phoon, K.K. (2017). Reliability evaluation of slope considering geological uncertainty and inherent variability of soil parameters. *Computers and Geotechnics*, *92*, 121–131.

[9] EN 1997-1: Eurocode 7. Geotechnical design. Part 1: General rules.

[10] Farah, K., Ltifi, M. & Hassis, H. (2015). A Study of probabilistic FEMs for a slope reliability analysis using the stress fields. *The Open Civil Engineering Journal*, *9*(1), 196–206.

[11] Fenton, G.A. & Griffiths, D.V. (2003). Bearing-capacity prediction of spatially random c-φ soils. *Canadian Geotechnical Journal*, *40*(1), 54–65.

[12] Griffiths, D.V. & Fenton, G.A. (2001). Bearing capacity of spatially random soil: The undrained clay Prandtl problem revisited. *Géotechnique*, *51*(4), 351–359.

[13] Huang, J., Lyamin, A.V., Griffiths, D.V., Sloan, S.W., Krabbenhoft, K. & Fenton, G.A. (2013). Undrained bearing capacity of spatially random clays by finite elements and limit analysis. Proceedings of the XVIII Int. Confer. on SMGE, 731-734.

[14] Jaksa, M.B., Kaggawa, W.S. & Brooker, P.I. (1999). Experimental evaluation of the scale of fluctuation of a stiff clay. ICASP-8 Conf. Proceedings, Sydney, Australia. Vol. 1, 415–422.

[15] Javankhoshdel, S. & Bathurst, R.J. (2015). Influence of cross correlation between soil parameters on probability of failure of simple cohesive and c-φ slopes. *Canadian Geotechnical Journal*, 2015-0109 (November),
[16] Ji, J., Zhang, C., Gao, Y. & Kodikara, J. (2018). Effect of 2D spatial variability on slope reliability: A simplified FORM analysis. *Geoscience Frontiers*, *9*(6), 1631–1638.
[17] Jiang, S.H., Li, D.Q., Zhang, L.M. & Zhou, C.B. (2014). Slope reliability analysis considering spatially variable shear strength parameters using a non-intrusive stochastic finite element method. *Engineering Geology*, *168*, 120–128.
[18] Jiang, S.H., Li, D.Q., Cao, Z.J., Zhou, C.B. & Phoon, K.K. (2015). Efficient system reliability analysis of slope stability in spatially variable soils using Monte Carlo Simulation. *Journal of Geotechnical and Geoenvironmental Engineering*, *141*(2), 04014096.
[19] Kim, J.M. & Sitar, N. (2013). Reliability approach to slope stability analysis with spatially correlated soil properties. *Soils and Foundations*, *53*(1), 1–10.
[20] Li, D.Q., Qi, X.-H., Cao, Z.-J., Tang, X.-S., Zhou, W., Phoon, K.-K. & Zhou, C.-B. (2015). Reliability analysis of strip footing considering spatially variable undrained shear strength that linearly increases with depth. *Soils and Foundations*, *55*(4), 866-880.
[21] Li, X.Y., Zhang, L.M., Gao, L. & Zhu, H. (2017). Simplified slope reliability analysis considering spatial soil variability. *Engineering Geology*, *216*, 90–97.
[22] Liu, L.L., Cheng, Y.M. & Zhang, S.H. (2017). Conditional random field reliability analysis of a cohesion-frictional slope. *Computers and Geotechnics*, *82*, 173–186.
[23] Liu, Y., Zhang, W., Zhang, L., Zhu, Z., Hu, J. & Wei, H. (2018). Probabilistic stability analyses of undrained slopes by 3D random fields and finite element methods. *Geoscience Frontiers*, *9*(6), 1657–1664.
[24] Lloret-Cabot, M., Fenton, G.A. & Hicks, M.A. (2014). On the estimation of scale of fluctuation in geostatistics. *Georisk:Assessment and Management of Risk for Engineered Systems and Geohazards*, *8*(2), 129–140.
[25] Low, B.K. & Phoon, K.K. (2015). Reliability based design and its complementary role to Eurocode 7 design approach. *Computers and Geotechnics*, *65*, 30-44.
[26] Oguz, E.A., Huvaj, N., & Griffiths, D.V. (2019). Vertical spatial correlation length based on standard penetration tests. *Marine Georesources & Geotechnology*, 37(1), 45-56.
[27] Ostoja-Starzewski, M. (2006). Material spatial randomness. From statistical to representative volume element. *Probabilistic Engineering Mechanics*, *21*, 112-132.
[28] Phoon, K.K. & Kulhawy, F.H. (1999a). Characterization of geotechnical variability. *Canadian Geotechnical Journal*, *36*(4), 612–624.
[29] Phoon, K.K. & Kulhawy, F.H. (1999b). Evaluation of geotechnical property variability. *Canadian Geotechnical Journal*, *36*(4), 625–639.
[30] Pieczyńska-Kozłowska, J.M., Puła, W. & Vessia, G. (2017). A collection of fluctuation scale values and autocorrelation functions of fine deposits in Emilia Romagna Palin, Italy. Geo-Risk 2017, ASCE Conf. Proceedings , Denver, USA, 360-369.
[31] Puła, W. & Chwała, M., (2015). On spatial averaging along random slip lines in the reliability computations of shallow strip foundations. *Computers and Geotechnics*, *68*, 128-136.
[32] Shen, Z., Jin, D., Pan, Q., Yang, H. & Chian, S.Ch. (2021). Effect of soil spatial variability on failure mechanisms and undrained capacities of strip foundations under uniaxial loading. *Computers and Geotechnics*, *139* (November), 104387.
[33] Tietje, O., Fitze, P. & Schneider, H.R. (2014). Slope stability analysis based on autocorrelated shear strength parameters. *Geotechnical and Geological Engineering*, *32*, 1477-1483.
[34] Vanmarcke, E.H. (2010). *Random Fields. Analysis and Synthesis*. World Scientific, Singapore. (rev. ed. of MIT Press, 1983).